

Chiral magnetization of non-Abelian vacuum: a lattice study

P. V. Buividovich^{a,b}, M. N. Chernodub^{c,d,b}, E. V. Luschevskaya^b, M. I. Polikarpov^b

^a*JINR "Sosny", National Academy of Science, Acad. Krasin str. 99, Minsk, 220109 Belarus*

^b*Institute for Theoretical and Experimental Physics, B. Cherenushkinskaya 25, Moscow, 117218 Russia*

^c*Laboratoire de Mathématiques et Physique Théorique, CNRS UMR 6083, Fédération Denis Poisson, Université de Tours, Parc de Grandmont, 37200, France*

^d*Department of Mathematical Physics and Astronomy, University of Gent, Krijgslaan 281, S9, B-9000 Gent, Belgium*

Abstract

The chiral magnetization properties of cold and hot vacua are studied using quenched simulations in lattice Yang-Mills theory. In weak external magnetic fields the magnetization is proportional to the first power of the magnetic field. We evaluate numerically the coefficient of the proportionality (the chiral susceptibility) using near-zero eigenmodes of overlap fermions. We found that the product of the chiral susceptibility and the chiral condensate equals to 46(3) MeV. This value is very close to the phenomenological value of 50 MeV. In strong fields the magnetization is a nonlinear function of the applied magnetic field. We find that the nonlinear features of the magnetization are well described by an inverse tangent function. The magnetization is weakly sensitive to temperature in the confinement phase.

Key words: Quantum Chromodynamics, lattice gauge theory, strong magnetic fields, chiral magnetization

PACS: 11.30.Rd, 12.38.Gc, 13.40.-f

1. Introduction

Quark is an electrically charged spin-1/2 particle with a magnetic moment. Following an analogy with electrodynamics [1], one can conclude that there exist at least two opposite types of the quark magnetic back-reaction of the QCD vacuum on the external magnetic field. The paramagnetic effect enhances magnetic field in the vacuum due to polarization of the magnetic moments of virtual quarks by the external magnetic field. On the contrary, the diamagnetic effect weakens the external field due to the (quantized) transverse orbital motion of the virtual quarks.

Qualitatively, there is a distant similarity of the QCD vacuum to a gas of electrically charged magnetic dipoles in electrodynamics [2]. However, there also is an important difference between QCD and electrodynamics: in the physically relevant limit of two massless quarks, QCD is classically conformal theory in which mass scale appears due to nonperturbative quantum effects. The response of the vacuum on the external magnetic fields is characterized by dimensionfull quantities and this feature makes the problem essentially nonperturbative.

In our paper we study, for the first time, the magnetization properties of the non-Abelian vacuum using numerical simulations in lattice gauge theory. The problem is not limited by academic interest, because very strong Abelian magnetic fields can be created, for example, in heavy ion collisions [3]. Such fields may substantially modify the phase diagram of QCD, changing even the order of the phase transition from the hadron phase to the quark-gluon plasma regime [4]. In lattice QCD the external field methods were already used to evaluate the electric polarizability of neutral mesons and baryons [5]. The dependence of the quark condensate on the strength of the uniform magnetic

field was also calculated recently in lattice gauge theory [6].

We concentrate on the (para)magnetic response of the vacuum which appears due to polarization of the spins (magnetic moments) of the virtual quarks and antiquarks in the external electromagnetic field. A natural quantitative measure of the spin polarization in the vacuum is given by the expectation value

$$\langle \bar{\Psi} \Sigma_{\alpha\beta} \Psi \rangle = \chi(F) \langle \bar{\Psi} \Psi \rangle q F_{\alpha\beta}, \quad (1)$$

where

$$\Sigma_{\alpha\beta} = \frac{1}{2i} [\gamma_{\alpha} \gamma_{\beta} - \gamma_{\beta} \gamma_{\alpha}], \quad (2)$$

is the relativistic spin operator, $F_{\alpha\beta}$ is the external electromagnetic field strength tensor and q is the electric charge of the quark Ψ . For simplicity, we omit flavor indices in (1) and consider it for one quark flavor.

The quantity (1) was first introduced by Ioffe and Smilga in Ref. [7] in order to analyze the nucleon magnetic moments which are related to phenomenologically interesting radiative transitions. Later the value of the magnetic susceptibility was estimated using various analytical approaches [8, 9, 10, 11]. The value of the magnetic susceptibility can be measured in experiments on lepton pair photoproduction through the chiral-odd coupling of a photon with quarks [12], and in radiative heavy meson decays [13].

The right hand side of Eq. (1) is proportional to the electromagnetic field strength tensor $F_{\mu\nu} = \partial_{\mu} a_{\nu} - \partial_{\nu} a_{\mu}$ due to the Lorenz covariance. The quark electric charge q appears in Eq. (1) since the electromagnetic field a_{μ} interacts with the quark field only in the combination $q a_{\mu}$. Another proportionality factor in the right hand side of Eq. (1) is the chiral condensate $\langle \bar{\Psi} \Psi \rangle$ (evaluated at the external electromagnetic field

F). This factor allows us to disentangle nonlinear effects of the enhancement of the chiral condensate in the external magnetic field [16, 6] from the effects of the quark's spin polarization.

In a leading order the magnetization of the QCD vacuum in weak magnetic fields should be a linear function of the field strength. Using perturbative QCD and the Schwinger proper time formalism one can show that the magnetization due to a strong magnetic field at one-loop order is proportional to $B \log B$ [14].

The strength of the vacuum polarization is characterized by a chiral magnetic susceptibility $\chi(F)$ in Eq. (1). In our discussion we treat the vacuum magnetization and the quark's spin polarization on equal footing skipping the g -factor which relates these quantities and characterizes the gyromagnetic ratio of the quarks.

The (chiral) magnetization of the QCD vacuum in the external magnetic field $B = F_{12} = -F_{21}$ can be described by the dimensionless quantity

$$\mu(qB) = \chi(qB) qB, \quad (3)$$

so that

$$\langle \bar{\Psi} \Sigma_{12} \Psi \rangle = \mu(qB) \langle \bar{\Psi} \Psi \rangle, \quad (4)$$

for the other Lorentz components the polarization (1) is zero. The quantity (3) is of central interest in our paper.

In Section 2 we derive an analytical formula which exactly relates the spinor structure of the low-lying Dirac eigenmodes to the magnetization (3). This formula is used to evaluate the magnetization numerically in Section 3. We discuss in details both the linear magnetization in a weak field and nonlinear features of this quantity in stronger fields. Our conclusions are summarized in the last Section.

2. A magnetization analog of Banks-Casher relation

In order to calculate the polarization properties of the QCD vacuum we derive the analytical formula which relates the magnetization to the spin structure of the low-lying quark eigenmodes. This formula is an analogue of the Banks-Casher relation [17]

$$\langle \bar{\Psi} \Psi \rangle = - \lim_{\lambda \rightarrow 0} \frac{\pi \rho(\lambda)}{V}, \quad (5)$$

which relates the chiral condensate $\langle \bar{\Psi} \Psi \rangle$ to the expectation value of the spectral density of the Dirac eigenmodes $\rho(\lambda)$ (to be defined below). In Appendix A we derive the Banks-Casher relation (5) in order to illustrate its relation to our analytical result (19).

The Euclidean partition function of QCD is given by the integral over the gluon fields A_μ^a , $\mu = 1, \dots, 4$ and $a = 1, \dots, N_c^2 - 1$, and over the quark Dirac fields Ψ_f , $f = 1, \dots, N_f$,

$$\begin{aligned} \mathcal{Z}_{\text{QCD}} &= \int \text{DA} \int \text{D}\Psi \int \text{D}\bar{\Psi} e^{-S_{\text{YM}}(A) - S_F(A, \Psi, \bar{\Psi})} \\ &\equiv \int \text{DA} \det[\mathcal{D}(A) + \mathcal{M}] e^{-S_{\text{YM}}(A)}, \end{aligned} \quad (6)$$

where S_{YM} is the Yang-Mills action. The fermion action is

$$S_F(A, \Psi, \bar{\Psi}) = \int d^4x \bar{\Psi}_f(x) [\mathcal{D}(A) + \mathcal{M}]_{ff'} \Psi_{f'}(x), \quad (7)$$

where \mathcal{M} is the $N_f \times N_f$ mass matrix in the flavor space.

For the sake of simplicity we consider below one fermion species ($N_f = 1$) with the mass m . Then $\mathcal{M} \equiv m$ and the fermion determinant in Eq. (6) is

$$F(m) = \det[\mathcal{D}(A) + m] \equiv \prod_k (i\lambda_k(A) + m), \quad (8)$$

where $\lambda_k = \lambda_k(A)$ is the eigenvalue of the massless Dirac operator $\mathcal{D} \equiv \gamma_\mu D_\mu$ in the background of the Euclidean gauge field configuration A . The spectrum of this operator is defined by the equation

$$\mathcal{D}\psi_k = i\lambda_k\psi_k, \quad (9)$$

where $\psi_k = \psi_k(x; A)$ is the corresponding eigenfunction (below we omit the argument “ A ” in ψ_k and λ_k for the sake of simplicity). Due to the anticommutation property, $\gamma_5 \mathcal{D} + \mathcal{D} \gamma_5 = 0$, any nonzero eigenvalue, $\lambda_k \neq 0$, comes in a pair with its opposite, $\lambda_{-k} = -\lambda_k$, corresponding to the eigenfunction $\psi_{-k} = \gamma_5 \psi_k$.

The eigenfunctions ψ_k form a basis in the spinor space: they are orthonormalized and complete (we always omit spinor indices),

$$\int d^4x \psi_k^\dagger(x) \psi_l(x) = \delta_{kl}, \quad (10)$$

$$\sum_k \psi_k(x) \psi_k^\dagger(x') = \delta(x - x'). \quad (11)$$

In the thermodynamic limit the expectation value of the magnetization (3) can be expressed via the nonzero eigenmodes, $\psi_k(x)$, of the massless Dirac operator (9).

$$\begin{aligned} -\langle \bar{\Psi} \Sigma_{\alpha\beta} \Psi \rangle &\equiv \langle \text{Tr} [\Sigma_{\alpha\beta} \Psi(x) \bar{\Psi}(x)] \rangle \\ &= \langle \text{Tr} [\Sigma_{\alpha\beta} D(x, x)] \rangle = \left\langle \sum_k \frac{\psi_k^\dagger(x) \Sigma_{\alpha\beta} \psi_k(x)}{i\lambda_k + m} \right\rangle \\ &= \left\langle \sum_{\lambda_k > 0} \frac{\psi_k^\dagger(x) \Sigma_{\alpha\beta} \psi_k(x)}{i\lambda_k + m} \right\rangle \\ &\quad + \left\langle \sum_{\lambda_k > 0} \frac{\psi_k^\dagger(x) \gamma_5 \Sigma_{\alpha\beta} \gamma_5 \psi_k(x)}{-i\lambda_k + m} \right\rangle, \end{aligned} \quad (12)$$

where the trace is taken over the spinor indices and the fermion propagator $D(x, x')$ is defined by Eq. (43). In the first row of Eq. (12) the notation $\langle \dots \rangle$ means the average over the gluon, A_μ , and fermion, Ψ , fields. After the integration over the fermion fields is done, the brackets $\langle \dots \rangle$ mean the average over gluon fields with the weight $F(m) e^{-S_{\text{YM}}(A)}$, where $F(m)$ is the determinant of the fermion operator (8). We omit the explicit dependence of the eigenfunctions λ_k and the eigenvalues ψ_k on the gluon field A_μ and the external electromagnetic field B . In the first row of Eq. (12) the minus sign appears due to anticommutative nature of the fermionic fields. Following the logic of the derivation of the Banks-Casher formula, we ignore in sums

over eigenvalues the exact zero modes, because the zero modes are inessential in the thermodynamic limit.

The spin operator (2) commutes with the γ_5 matrix,

$$\gamma_5 \Sigma_{\alpha\beta} - \Sigma_{\alpha\beta} \gamma_5 = 0, \quad (13)$$

so that $\gamma_5 \Sigma_{\alpha\beta} \gamma_5 = \Sigma_{\alpha\beta}$ because $\gamma_5^2 = 1$. Then Eq. (12) gives us the following expression for the magnetization:

$$\langle \bar{\Psi} \Sigma_{\alpha\beta} \Psi \rangle = 2m \left\langle \sum_{\lambda_k > 0} \frac{\psi_k^\dagger(x) \Sigma_{\alpha\beta} \psi_k(x)}{\lambda_k^2 + m^2} \right\rangle. \quad (14)$$

Similarly to the derivation of the Banks-Casher relation (Appendix A) we take the limit $m \rightarrow 0$ and get

$$\langle \bar{\Psi} \Sigma_{\alpha\beta} \Psi \rangle = 2\pi \left\langle \int_0^\infty d\lambda \nu(\lambda) \delta(\lambda) \psi_\lambda^\dagger(x) \Sigma_{\alpha\beta} \psi_\lambda(x) \right\rangle, \quad (15)$$

where $\nu(\lambda)$ is the spectral density of the Dirac eigenvalues,

$$\rho(\lambda) = \langle \nu(\lambda) \rangle, \quad \nu(\lambda) = \sum_k \delta(\lambda - \lambda_k). \quad (16)$$

Then we take the average of this expression over the whole space-time and take the integral over λ

$$\langle \bar{\Psi} \Sigma_{\alpha\beta} \Psi \rangle = \lim_{\lambda \rightarrow 0} \left\langle \frac{\pi \nu(\lambda)}{V} \int d^4x \psi_\lambda^\dagger(x) \Sigma_{\alpha\beta} \psi_\lambda(x) \right\rangle. \quad (17)$$

Note, that if in Eq. (17) we take the unit operator $\mathbb{1}$ instead of the spin operator $\Sigma_{\alpha\beta}$ then we immediately recover the Banks-Casher formula (5) due to the normalization condition (10).

In Appendix B we give some arguments in favor of the validity of the factorization (17). Then, using (5), we get:

$$\langle \bar{\Psi} \Sigma_{\alpha\beta} \Psi \rangle = \langle \bar{\Psi} \Psi \rangle \left\langle \int d^4x \psi_\lambda^\dagger(x) \Sigma_{\alpha\beta} \psi_\lambda(x) \right\rangle. \quad (18)$$

Our sketch of the proof of factorization property (18) in Appendix B is valid in infinite volume. In the next Section we check numerically the factorization in our finite volumes as well.

Having compared Eq. (18) with the definition for the magnetic susceptibility χ_m in Eq. (1), we get

$$\chi(qF) qF_{\alpha\beta} = - \lim_{\lambda \rightarrow 0} \left\langle \int d^4x \psi_\lambda^\dagger(x; F) \Sigma_{\alpha\beta} \psi_\lambda(x; F) \right\rangle. \quad (19)$$

Here $\psi_\lambda(x; F)$ is the eigenmode of the Dirac operator in the external (magnetic) background field $B = F_{12}$. Next, we use the definition (3) of the magnetization μ to rewrite Eq. (19) as follows

$$\mu(qB) = - \lim_{\lambda \rightarrow 0} \left\langle \int d^4x \psi_\lambda^\dagger(x; B) \Sigma_{12} \psi_\lambda(x; B) \right\rangle. \quad (20)$$

This is our final analytical expression which we use for the evaluation of the magnetization in our numerical simulations.

Eq. (18) demonstrates the apparent factorization of the chiral condensate in line with the original definition (1) of Ref. [7]. Due to the factorization (18) the chiral condensate does not enter explicitly our final formulas (19) and (20), and therefore one can hope that various ambiguities (related to the definition and/or logarithmic divergence of the condensate in the quenched limit) does not enter our definition of the magnetization.

Table 1: Parameters of simulations.

L_s	L_t	β	a , fm	V_{3d} , fm ³	T/T_c
14	14	3.2810	0.103	1.44 ³	0
16	16	3.2810	0.103	1.65 ³	0
16	16	3.3555	0.089	1.42 ³	0
16	6	3.1600	0.128	2.01 ³	0.82

3. Magnetization from first principles

3.1. Numerical simulations

We simulate lattice SU(2) Yang-Mills theory with tadpole-improved Symanzik action for the gauge fields [18]. This improvement provides us with smoother gauge configurations compared to the usual Wilson action. The fermionic eigenmodes are calculated using the overlap Dirac operator for quarks in the fundamental representation [19]. One of the most important advantages of the overlap Dirac operator is its explicit chiral symmetry at all lattice spacings. Basically, we used the same technique as was implemented in Ref. [20].

In our quenched simulations we calculated the magnetization of the d -quark condensate which has the smallest (absolute value of) the electric charge $q = |q| = e/3$. In continuum notations, the uniform magnetic field in the third spatial direction is introduced into the Dirac operator by shifting the non-Abelian vector potential A_μ by the singlet Abelian potential a_μ :

$$\begin{aligned} A_\mu^{ij} &\rightarrow A_\mu^{ij} + a_\mu \delta^{ij}, \\ a_\mu &= B/2 (x_2 \delta_{\mu 1} - x_1 \delta_{\mu 2}). \end{aligned} \quad (21)$$

In order to adopt the field (21) to a finite volume with periodic boundary conditions we have introduced an additional x -dependent boundary twist for fermions following Ref. [21]. In a finite spatial volume L^3 with periodic boundary conditions the total magnetic flux through any two-dimensional face L^2 of the lattice cube should be quantized [22]. This condition leads to the quantization of the uniform magnetic field:

$$qB = \frac{2\pi k}{L^2}, \quad k \in \mathbb{Z}. \quad (22)$$

The physical strength of the magnetic field is a periodic function of the flux number k with the period L^2 . The maximal strength is reached at $k = L^2/2$.

The parameters of our simulations are given in Table I. For $T = 0$ we used three lattice volumes and two values of the lattice spacing a in order to check the systematic errors due to finite volume and finite lattice spacing. In our simulations we used 20 gauge field configurations for each set of parameters given in Table I. We make simulations at zero temperature and at $T = 0.82T_c$. The critical temperature in SU(2) gauge theory is $T_c = 313.(3)$ MeV [23]. We evaluate the limit $\lambda \rightarrow 0$ in (20) by averaging this expression over low-lying nonzero Dirac eigenmodes with eigenvalues in the interval $[0 \dots 50 \text{ MeV}]$. In order to evaluate the magnetization we use the asymptotic formula (20) which is based on the factorization property (18).

This approach is valid in the thermodynamic and chiral limits, taken simultaneously.

We show the magnetization at zero temperature as the function of the external magnetic field in Figure 1. The values of

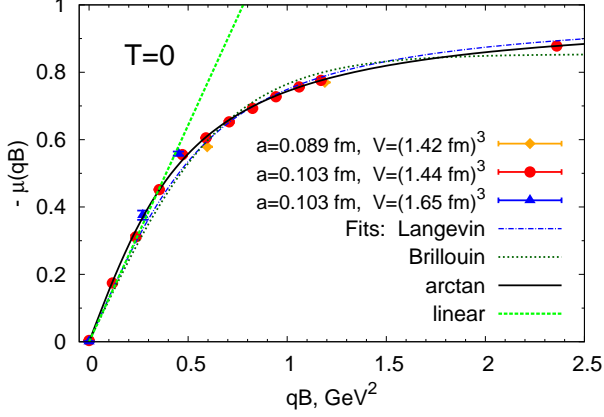


Figure 1: The magnetization μ as a function of the strength of the external magnetic field qB at zero temperature. The lattice spacings and spatial volumes are shown for all data sets. The fits are discussed in the text.

the magnetization obtained at different spatial volumes and different lattice spacings are very close to each other. The relative discrepancies are much smaller than, e.g., for the values of the chiral condensate [6]. This fact indicates finite-volume and finite-spacing dependencies of bilinear fermionic operators cancel in (4) with a good precision.

In Figure 2 we have also checked that the factorization property (18) is established very well for all checked strengths of the magnetic field. The values of the magnetization, evaluated with the help of the original (14) and factorized (20) definitions agree with each other within error bars. Unfortunately, the nonfactorized definition (14) gives us much larger error bars compared to the factorized definition (20) at the same statistics. Therefore below we use the factorized definition only.

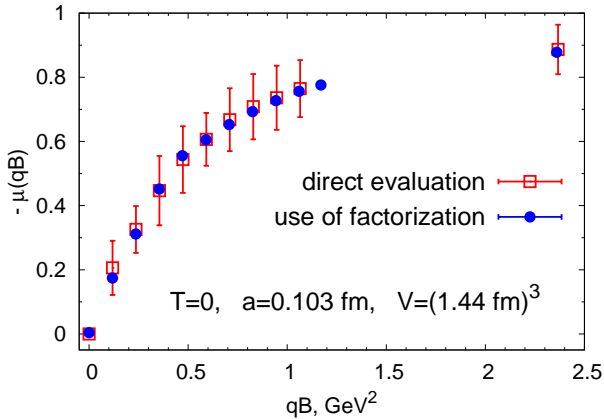


Figure 2: The check of the factorization property for the magnetization μ . The magnetization is calculated using both the original (14) and the factorized (20) definitions (shown as the empty squares and the full circles, respectively).

The behavior of the magnetization is consistent with general expectations: at low magnetic fields the magnetization is linear.

This fact indicates the existence of a nonzero susceptibility at vanishingly small external magnetic field confirming the presence of the paramagnetic contribution due to the quark's spin. At high magnetic fields the quarks ensembles should be fully polarized so that the magnetization should come to a saturation regime. Mathematically, in Eq. (20) at strong magnetic fields the lowest-lying eigenfunctions with $m = +1$ eigenvalue of the spin projection operator Σ_{12} become dominated over the eigenfunctions with the $m = -1$ eigenvalue, thus leading to the full polarization of the eigenmodes. In our units the saturation condition is to be as follows:

$$\lim_{qB \rightarrow \infty} \mu(qB) = -1. \quad (23)$$

Figure 1 supports this observation.

In Figure 3 we compare our zero-temperature data with the finite temperature magnetization obtained at $T = 0.82T_c$. Visually, the effect of the temperature on magnetization is rather

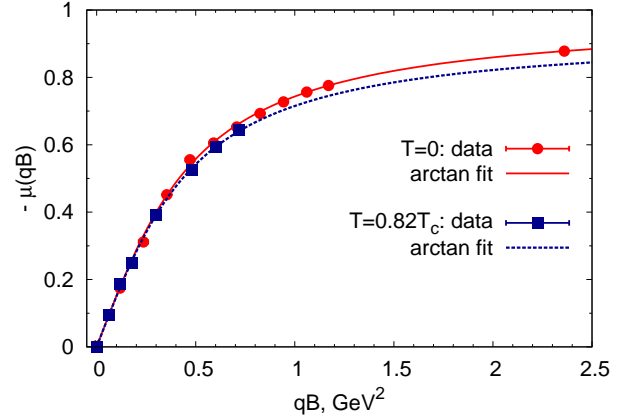


Figure 3: The magnetization μ as a function of the strength of the magnetic field, qB at $T = 0$ (14^4 lattice) and $T = 0.82T_c$ ($16^3 \times 6$ lattice). Best arctan-based fits (30) with two fitting parameters are shown.

small. More detailed analysis of $T = 0$ and $T > 0$ data will be done in the next subsection.

3.2. Analysis of magnetization

Let us compare our results with well known expressions for simple paramagnetic systems. The specific (i.e., per atom) magnetization of a classical ideal paramagnetic gas is given by [2]

$$\mu^{\text{class}}(B) = \mu \left[\coth \alpha(B) - \frac{1}{\alpha(B)} \right], \quad (24)$$

$$\alpha(B) = \frac{\mu B}{k_B T}, \quad (25)$$

where μ is the magnetic moment of a single molecule, T is temperature and k_B is the Boltzmann constant. The function in the brackets in Eq. (24) is often called the Langevin function.

The quantum analogue of the Langevin function (24) for a spin 1/2-particle is described by the Brillouin behavior [24]:

$$\mu^{\text{quant}}(B) = \mu [2 \coth 2\alpha(B) - \coth \alpha(B)]. \quad (26)$$

The atoms are supposed to be electrically neutral otherwise the paramagnetic magnetization – either classical (24) or quantum (26) – should be supplemented by a diamagnetic contribution due to Landau quantization (the motion of the atoms in transverse direction to the magnetic field is to be constrained to the Landau levels). In an electron gas the diamagnetic contribution provides an essential part of the total magnetization [1]. However, we do not consider the diamagnetic contribution of the quark’s motion because of the paramagnetic nature of the condensate (1).

A similar behavior of the magnetization (24) and (26) is also provided by inverse tangent function which we add here for completeness:

$$\mu^{\text{trig}}(B) = \frac{2\mu}{\pi} \arctan \alpha(B). \quad (27)$$

At weak magnetic fields all functions (24), (26) and (27) are linear in the magnetic field. At strong magnetic field all expressions for the magnetization are consistent with the saturation property (23).

In the examples (24), (26) and (27) the temperature T enters the magnetization via Eq. (25). The temperature plays a role of the disorder ingredient which diminishes the magnetization of the system. In our simulations the disorder factor is coming – even at the zero-temperature case – from the random fluctuating background of the non-Abelian gauge fields, making the temperature T to be an effective parameter in all considered examples.

We fit our data by three functions inspired by Eqs. (27), (24) and (26):

$$\mu_{\text{fit}}^{\text{class}}(B) = \mu_{\infty} \left[\coth \frac{3\chi_0 qB}{\mu_{\infty}} - \frac{\mu_{\infty}}{3\chi_0 qB} \right], \quad (28)$$

$$\mu_{\text{fit}}^{\text{quant}}(B) = \mu_{\infty} \left[2 \coth \frac{2\chi_0 qB}{\mu_{\infty}} - \coth \frac{\chi_0 qB}{\mu_{\infty}} \right], \quad (29)$$

$$\mu_{\text{fit}}^{\text{trig}}(B) = \frac{2\mu_{\infty}}{\pi} \arctan \frac{\pi\chi_0 qB}{2\mu_{\infty}}. \quad (30)$$

These fitting functions share the following properties. All these fitting functions are the functions of the two parameters: the zero-field susceptibility χ_0 and the strong-field saturation constant, μ_{∞} . Indeed, in weak and strong field limits one gets, respectively

$$\mu_{\text{fit}}^i(B) = \chi_0 \cdot qB + \dots \quad \text{as } qB \rightarrow 0; \quad (31)$$

and [25]

$$\lim_{qB \rightarrow \infty} \mu_{\text{fit}}^i(qB) = -\mu_{\infty}. \quad (32)$$

Here the index i stands for the type of the fitting function: “class”, “quant” or “trig”.

According to Eq.(23) we expect that

$$\mu_{\infty} = 1. \quad (33)$$

Thus we fit the data using the functions (28), (29) and (30) with χ_0 and μ_{∞} being the two fitting parameters. We also perform an additional set of one-parameter fits with fixed $\mu_{\infty} = 1$. Finally,

we also fit the weak-field behavior of the magnetization by the linear function (31).

The fitting results are presented in Tables 2 and 3 for zero and non-zero temperature cases, respectively.

Table 2: Fitting results at $T = 0$.

fits	$-\chi_0, \text{GeV}^{-2}$	μ_{∞}	$\chi^2/\text{d.o.f.}$
one parameter fits			
linear	1.42(6)	-	25
arctan	1.43(1)	1	285
Langevin	1.22(2)	1	10^4
Brillouin	0.71(6)	1	$6 \cdot 10^5$
two parameter fits			
arctan	1.547(6)	0.985(7)	7.2
Langevin	1.37(2)	0.976(2)	73
Brillouin	1.06(3)	0.883(4)	10^3

Table 3: Fitting results at $T = 0.82T_c$.

fits	$-\chi_0, \text{GeV}^{-2}$	μ_{∞}	$\chi^2/\text{d.o.f.}$
one parameter fits			
linear	1.46(6)	-	1.8
arctan	1.46(2)	1	1.05
Langevin	1.36(4)	1	3.8
Brillouin	1.19(6)	1	17.6
two parameter fits			
arctan	1.53(3)	0.94(2)	0.57
Langevin	1.49(4)	0.87(2)	0.71
Brillouin	1.47(4)	0.71(2)	1.1

At $T = 0$ all fits have quite large values of $\chi^2/\text{d.o.f.}$, Table 2. The lowest value of this important quantity is reached for the arctan fitting function (30) with two fitting parameters. Notice that both for the arctan-based (30) function and for the classical Langevin (28) fitting function the asymptotic values of the polarization μ_{∞} are very close to the theoretical expectation (33).

At $T = 0$ the quantum (Brillouin) function (29) does not work at all: it has the very large value of $\chi^2/\text{d.o.f.}$ and the strong-field limit is also inconsistent with our expectation (33). The fitting functions – corresponding to the one-parameter fits – are shown in Figure 1 by lines.

We point out that the linear fit at the weak field limit does not agree with most other fitting functions. The linear fitting is done for the relatively weak magnetic fields, $0 \leq \sqrt{qH} \leq 500 \text{ MeV}$ (shown as a straight line in Figure 1). The fields from this interval, however, are of the order or even higher than typical QCD scale $\Lambda_{\text{QCD}} \sim 200 \text{ MeV}$. Therefore, the nonlinear effects may affect the determination of the zero-field susceptibility if the fitting is done by the linear function. Below we quote the result for the magnetic susceptibility using the arctan-based (30) function. The corresponding value is presented in the bold font in Table 2.

In a finite volume the physical magnetic field (22) is a periodic function of the number of elementary magnetic fluxes k

going through any face of the lattice volume [22]. Since the periodic finite-volume behavior at very strong fields is not reflected in the form of the fitting functions (28), (29) and (30) the asymptotic magnetization μ_∞ of two-parameter fits may deviate from the expected high-field limit (33). However, the artifacts related to the finite volume of the lattice are small since for the best fits by the functions (28) and (30) the deviations from the limit (33) are small. We also note that the logarithmic effects – predicted in Ref. [14] – cannot be reliably determined from our data because of the coarse grid of the data points at strong fields.

At $T = 0.82T_c$ the fits have more reasonable values of $\chi^2/\text{d.o.f.}$, Table 3. The error bars of the best fit parameters are larger so that the zero-field susceptibility agrees within error bars for almost all the fitting functions except for the Brillouin function (29). The best fit – in terms of both the quality of the fit and the value of the asymptotic polarization μ_∞ , Eq. (33) – is the arctan-based (30) function. The accepted value is given in the bold font in Table 3. Finally, the linear fitting is done in the range $0 \leq \sqrt{qH} \leq 0.425\text{MeV}$.

The best two parameter arctan-fits for both values of temperature are shown in Figure 3 by lines along with the data. The magnetic susceptibility turns out to be insensitive with respect to the variation of the temperature:

$$\chi_0 = \begin{cases} -1.547(6) \text{ GeV}^{-2} & T = 0 \\ -1.53(3) \text{ GeV}^{-2} & T = 0.82T_c \end{cases} \quad (34)$$

Our lattice spacings, $a = \Lambda_{\text{UV}}^{-1}$, correspond to the scales $\Lambda_{\text{UV}}(T = 0) \sim 2 \text{ GeV}$ and $\Lambda_{\text{UV}}(T = 0.82 T_c) \sim 1.5 \text{ GeV}$, respectively. Other estimations of the chiral susceptibility were done in [7, 8, 9, 10, 11, 13, 15].

Theoretically, the value of the magnetic susceptibility can be parameterized in the form [9]

$$\chi = -\frac{c_\chi N_c}{8\pi^2 f_\pi^2}, \quad (35)$$

where c_χ is a dimensionless parameter and $f_\pi = 130.7 \text{ MeV}$ is the pion decay constant for $N_c = 3$.

In the notations of Eq. (35) the result of our calculation (34) at $T = 0$ corresponds to

$$c_\chi(T = 0) = 1.043(4). \quad (36)$$

The operator product expansion combined with the pion dominance idea gives us the value $c_\chi = 2$ [9]. The corresponding theoretical prediction for $SU(2)$ gauge theory is

$$\chi(T = 0) = -2.97 \text{ GeV}^{-2} \quad (\text{for } N_c = 2). \quad (37)$$

The holographic description of QCD gives a slightly higher value for the susceptibility, $c_\chi = 2.15$ [10]. Both the results of Refs. [9] and [10] agree well with the original QCD sum rule fit made by Ioffe and Smilga [7].

In the instanton liquid model of the QCD vacuum the magnetic susceptibility was first calculated in Ref. [11]. After a proper rescaling we obtain the value $c_\chi = 1.24$ corresponding to the instanton model.

Thus, our zero-temperature result (34), (36) is by 25% smaller than the value of the magnetic susceptibility obtained in the instanton vacuum [11], and is by a factor of two smaller than the value obtained by traditional field theoretic and modern holographic approaches. These discrepancies are not unexpected since we used the quenched lattice study in which all vacuum quark loops are ignored, and the anomalous dimension of the chiral susceptibility was not taken into account. Moreover, our calculations are performed in the $SU(2)$ gauge theory in which the number of colors is reduced in comparison with the real QCD.

An experimentally relevant and phenomenologically interesting quantity is given by the product of the chiral susceptibility χ and the chiral condensate $\langle \bar{\Psi}\Psi \rangle$ [12]. Using our zero-temperature result for the chiral susceptibility (34) and the value for the chiral condensate obtained in other quenched studies [6, 20], $\langle \bar{\Psi}\Psi \rangle = [310(6) \text{ MeV}]^3$, one gets

$$-\chi \langle \bar{\Psi}\Psi \rangle = 46(3) \text{ MeV} \quad [\text{quenched limit}]. \quad (38)$$

This result is surprisingly close to the estimation based on the QCD sum rules techniques, which gives for (38) the number of the order of 50 MeV [8].

4. Conclusions

We have evaluated for the first time the magnetic susceptibility of the chiral condensate using the first-principle methods of lattice $SU(2)$ gauge theory in the quenched limit. To this end we have derived formula (19) which relates the chiral magnetization of the QCD vacuum to the low-lying chiral eigenmodes of the Dirac operator in a manner of the Banks-Casher relation (the exact zero modes do not contribute to the magnetization in the thermodynamic limit). In order to derive Eq. (19) we used the factorization property (18), which was verified numerically. We calculated these eigenmodes using the overlap fermion operator in the background of gluon fields generated with the help of the tadpole-improved Symanzik action.

We found that at weak magnetic field the magnetization of the QCD vacuum is a linear function of the field strength. The associated chiral magnetic susceptibility is almost independent on temperature (34) up to $T = 0.82 T_c$. The value of the magnetization (34) is smaller compared to the existing analytical estimates (37) for $SU(2)$ gauge theory. We attribute the reason for the difference to the quenching effects.

The nonlinear features of the magnetization are very well described by an inverse tangent function (30) of the applied magnetic field, Figure 3. This parametrization of the magnetization works both at zero and non-zero temperatures in the confinement phase.

Acknowledgments

The authors are grateful to Ph. Boucaud, V.G. Bornyakov, V.V. Braguta, A.S. Gorsky, B.L. Ioffe, B.O. Kerbikov, D. Kharzeev, A. Krikun, S.M. Morozov, V.A. Novikov,

V.I. Shevchenko, M.I. Vysotsky, and V.I. Zakharov for interesting discussions. We thank B. Pire for making us aware of Ref. [12]. This work was partly supported by Grants RFBR No. 08-02-00661-a, grant for scientific schools No. NSh-679.2008.2, by the Russian Federal Agency for Nuclear Power, and by the STINT Institutional grant IG2004-2 025. P.V.B. is also partially supported by the Euler scholarship from DAAD, by a scholarship of the Dynasty Foundation and by the grant BRFB F08D-005 of the Belarusian Foundation for Fundamental Research. E.V.L. is partially supported by grant for scientific schools No Nsh-4961.2008.2 and grants RFBR 06-02-17012 and 09-02-00629. The calculations were partially done on the MVS 50K at Moscow Joint Supercomputer Center.

A. Banks-Casher relation: chiral condensate via eigenmodes

In Section 2 the relation of the magnetization to the Dirac eigenmodes was shown to be given by Eq. (19). For the sake of completeness we present below a derivation of the Banks-Casher relation [17] which is very similar to the derivation of Eq. (19).

A differentiation of the partition function (6) with respect to the mass m in the thermodynamic limit provides us with the chiral condensate,

$$\langle \bar{\Psi}\Psi \rangle = -\frac{1}{V} \frac{\partial}{\partial m} \ln \mathcal{Z}_{QCD} = -\frac{1}{V} \left\langle \sum_{\lambda_k > 0} \frac{2m}{\lambda_k^2 + m^2} \right\rangle, \quad (39)$$

where we have used Eq. (8) as well as the pairwise appearance of the mutually opposite eigenvalues,

$$\frac{1}{F(m)} \frac{\partial F(m)}{\partial m} = \sum_{\lambda_k} \frac{1}{i\lambda_k + m} = \sum_{\lambda_k > 0} \frac{2m}{\lambda_k^2 + m^2}. \quad (40)$$

The zero mode(s), corresponding to $\lambda_0 = 0$, are not counted in Eq. (40) because they give vanishing contribution in the thermodynamic limit, and thus are irrelevant.

In the chiral limit, $m \rightarrow 0$, Eq. (39) provides us with the celebrated Banks-Casher formula [17], Eq. (5), which relates the chiral condensate $\langle \bar{\Psi}\Psi \rangle$ to the expectation value $\rho(\lambda)$ of the spectral density $\nu(\lambda)$ of the Dirac eigenvalues (16) in the limit to zero virtuality, $\lambda \rightarrow 0$. In order to derive Eq. (5) we have used the relations

$$\lim_{m \rightarrow 0} \frac{1}{\pi} \frac{m}{\lambda^2 + m^2} = \delta(\lambda) \quad \text{and} \quad \int_0^\infty d\lambda \delta(\lambda) = \frac{1}{2}, \quad (41)$$

so that

$$\begin{aligned} \sum_{\lambda_k > 0} \frac{2m}{\lambda_k^2 + m^2} &= \int_0^\infty d\lambda \nu(\lambda) \frac{2m}{\lambda^2 + m^2} \\ &\xrightarrow{m \rightarrow 0} 2\pi \int_0^\infty d\lambda \nu(\lambda) \delta(\lambda) = \pi \lim_{\lambda \rightarrow 0} \nu(\lambda). \end{aligned} \quad (42)$$

The fermionic propagator in the background of the gauge field A_μ can be expressed in terms of the eigenmodes (9) as follows:

$$\langle \Psi(x) \bar{\Psi}(x') \rangle_A \equiv D(x, x') = \sum_k \frac{\psi_k(x) \psi_k^\dagger(x')}{i\lambda_k + m}. \quad (43)$$

Due to the completeness condition (11) the propagator (43) satisfies the equation

$$[\mathcal{D}(A) + m] D(x, x') = \delta(x - x'). \quad (44)$$

B. Factorization in Eq. (18)

Below discuss a possible origin of the factorization in Eqs. (17) and (18), which was used to evaluate the chiral susceptibility in this article. Consider two local operators, $\mathcal{O}_1(x)$ and $\mathcal{O}_2(x)$, which are functions of the lattice coordinate x . Then in infinite volume limit

$$\left\langle \frac{1}{V} \sum_x \mathcal{O}_1(x) \mathcal{O}_2(y) \right\rangle = \langle \mathcal{O}_1 \rangle \langle \mathcal{O}_2 \rangle. \quad (45)$$

The proof of (45) is trivial, since the quantum average in lattice calculations is equivalent to a sum over infinite number of gauge field configurations:

$$\begin{aligned} \left\langle \frac{1}{V} \sum_x \mathcal{O}_1(x) \mathcal{O}_2(y) \right\rangle &= \lim_{N_{\text{conf}} \rightarrow \infty} \sum_{i=1}^{N_{\text{conf}}} \frac{1}{V} \sum_x \mathcal{O}_1(x) \mathcal{O}_2(y), \end{aligned} \quad (46)$$

where V is the number of lattice points x , and the sum in (46) goes over gauge field configurations labeled by the index i . The gauge field configurations are generated with the Boltzmann probability density $e^{-S_{YM}(A)}/\mathcal{Z}$. For infinite volume, $V \rightarrow \infty$, the average for one gauge field configuration is equal to the quantum average,

$$\frac{1}{V} \sum_x \mathcal{O}_1(x) = \langle \mathcal{O}_1(x) \rangle. \quad (47)$$

Equation (45) follows from Eqs. (46) and (47).

If one takes $\mathcal{O}_1(x) = \mathcal{O}_2(x) = \text{Tr} F_{\mu\nu}^2(x)$, then in the continuum limit we get from Eq. (45) the well known factorization formula:

$$\lim_{V \rightarrow \infty} \left\langle \frac{1}{V} \int d^4x \text{Tr} F_{\mu\nu}^2(x) \text{Tr} F_{\mu\nu}^2(y) \right\rangle = \langle \text{Tr} F_{\mu\nu}^2 \rangle^2. \quad (48)$$

The factorization of the magnetization, Eqs. (17) and (18), is very similar to the factorization (45). We only have to prove that the analogue of Eq. (47) is valid for the bulk quantities $\lim_{\lambda \rightarrow 0} \pi \nu(\lambda)/V$ and $\lim_{\lambda \rightarrow 0} \int d^4x \psi_\lambda^\dagger(x) \Sigma_{\alpha\beta} \psi_\lambda(x)$. One can naturally assume that these quantities have a smooth behavior towards the continuum limit, $V \rightarrow \infty$. Then the average over one infinitely large configuration of the gauge fields is equal to the usual quantum average of the factorized expression, and then the factorization (18) is valid.

References

- [1] L.D. Landau and E.M. Lifshitz, Statistical Physics Part I, vol. 5 of Course of Theoretical Physics (Pergamon Press, Oxford, 1980).
- [2] H. P. Myers, "Introductory solid state physics" (CRC Press, New York, 1997).
- [3] D. E. Kharzeev, L. D. McLerran and H. J. Warringa, Nucl. Phys. A **803**, 227 (2008) [arXiv:0711.0950 [hep-ph]]; I. V. Selyuzhenkov [STAR Collaboration], Rom. Rep. Phys. **58**, 049 (2006) [arXiv:nucl-ex/0510069]; V. Skokov, A. Illarionov and V. Toneev, arXiv:0907.1396 [nucl-th]; J. Rafelski, L. P. Fulcher and A. Klein, Phys. Rept. **38**, 227 (1978).
- [4] N. O. Agasian and S. M. Fedorov, Phys. Lett. B **663**, 445 (2008) [arXiv:0803.3156 [hep-ph]]; E. S. Fraga and A. J. Mizher, Phys. Rev. D **78**, 025016 (2008) [arXiv:0804.1452 [hep-ph]].
- [5] H. R. Fiebig, W. Wilcox and R. M. Woloshyn, Nucl. Phys. B **324**, 47 (1989); J. C. Christensen, W. Wilcox, F. X. Lee and L. m. Zhou, Phys. Rev. D **72**, 034503 (2005) [arXiv:hep-lat/0408024]; W. Detmold, B. C. Tiburzi and A. Walker-Loud, Phys. Rev. D **79**, 094505 (2009) [arXiv:0904.1586 [hep-lat]].
- [6] P. V. Buividovich, M. N. Chernodub, E. V. Luschevskaya and M. I. Polikarpov, arXiv:0812.1740 [hep-lat].
- [7] B. L. Ioffe and A. V. Smilga, Nucl. Phys. B **232**, 109 (1984).
- [8] I. I. Balitsky and A. V. Yung, Phys. Lett. B **129**, 328 (1983); V. M. Belyaev and Y. I. Kogan, Yad. Fiz. **40**, 1035 (1984); I. I. Balitsky, A. V. Kolesnichenko and A. V. Yung, Sov. J. Nucl. Phys. **41**, 178 (1985) [Yad. Fiz. **41**, 282 (1985)]; P. Ball, V. M. Braun and N. Kivel, Nucl. Phys. B **649**, 263 (2003) [arXiv:hep-ph/0207307].
- [9] A. Vainshtein, Phys. Lett. B **569**, 187 (2003) [arXiv:hep-ph/0212231].
- [10] A. Gorsky and A. Krikun, arXiv:0902.1832 [hep-ph].
- [11] H. C. Kim, M. Musakhanov and M. Siddikov, Phys. Lett. B **608**, 95 (2005) [arXiv:hep-ph/0411181].
- [12] V. M. Braun, S. Gottwald, D. Y. Ivanov, A. Schafer and L. Szymanowski, Phys. Rev. Lett. **89**, 172001 (2002) [arXiv:hep-ph/0206305]; B. Pire and L. Szymanowski, Phys. Rev. Lett. **103**, 072002 (2009) [arXiv:0905.1258].
- [13] J. Rohrwild, JHEP **0709**, 073 (2007) [arXiv:0708.1405 [hep-ph]].
- [14] T. D. Cohen and E. S. Werbos, Phys. Rev. C **80**, 015203 (2009) [arXiv:0810.5103 [hep-ph]].
- [15] B. L. Ioffe, Phys. Lett. B **678**, 512 (2009) [arXiv:0906.0283].
- [16] I. A. Shushpanov and A. V. Smilga, Phys. Lett. B **402**, 351 (1997) [arXiv:hep-ph/9703201].
- [17] T. Banks and A. Casher, Nucl. Phys. B **169**, 103 (1980).
- [18] M. G. Alford, W. Dimm, G. P. Lepage, G. Hockney and P. B. Mackenzie, Phys. Lett. B **361**, 87 (1995) [arXiv:hep-lat/9507010]; V. G. Bornyakov, E. M. Ilgenfritz and M. Mueller-Preussker, Phys. Rev. D **72**, 054511 (2005) [arXiv:hep-lat/0507021].
- [19] H. Neuberger, Phys. Lett. B **417**, 141 (1998).
- [20] P. V. Buividovich, E. V. Luschevskaya and M. I. Polikarpov, Phys. Rev. D **78**, 074505 (2008) [arXiv:0809.3075 [hep-lat]].
- [21] M. H. Al-Hashimi and U. J. Wiese, arXiv:0807.0630.
- [22] P. H. Damgaard and U. M. Heller, Nucl. Phys. B **309**, 625 (1988).
- [23] V.G. Bornyakov, E.M. Ilgenfritz, B.V. Martemyanov, S.M. Morozov, M. Muller-Preussker, A.I. Veselov, Phys. Rev. D **76**, 054505 (2007) [arXiv:0706.4206 [hep-lat]].
- [24] Here μ and α have different normalizations compared to the ones used in Eq. (24). This remark plays no role in our discussion below since we are interested only in the general functional behavior of the magnetization.
- [25] The minus sign appears in the right hand side of Eq. (32) because the weak-field susceptibility is negative, $\chi_0 < 0$.